

# Nuclear Envelope Breakdown Requires Overcoming the Mechanical Integrity of the Nuclear Lamina\*<sup>[S]</sup>

Received for publication, May 4, 2004, and in revised form, July 7, 2004  
Published, JBC Papers in Press, July 30, 2004, DOI 10.1074/jbc.M402474200

Porntula Panorchan<sup>‡</sup>, Benjamin W. Schafer<sup>§</sup>, Denis Wirtz<sup>‡¶||</sup>, and Yiider Tseng<sup>‡\*\*</sup>

From the Departments of <sup>‡</sup>Chemical and Biomolecular Engineering, <sup>§</sup>Civil Engineering, and <sup>¶</sup>Materials Science and Engineering, The Johns Hopkins University, Baltimore, Maryland 21218

**In prophase cells, lamin B1 is the major component of the nuclear lamina, a filamentous network underlying the nucleoplasmic side of the nuclear membrane, whereas lamin A/C is dissociated from the scaffold. *In vivo* fluorescence microscopy studies have shown that, during the G<sub>2</sub>/M transition, the first gap in the nuclear envelope (NE) appears before lamin B1 disassembly and is caused by early spindle microtubules impinging on the NE. This result suggests that the mechanical tearing of the NE by microtubules plays a central role to the progression of mitosis. To investigate whether this microtubule-induced NE deformation is sufficient for NE breakdown, we assess the mechanical resilience of a reconstituted lamin B1 network. Quantitative rheological methods demonstrate that human lamin B1 filaments form stiff networks that can resist much greater deformations than those caused by microtubules impinging on the NE. Moreover, lamin B1 networks possess an elastic stiffness, which increases under tension, and an exceptional resilience against shear deformations. These results demonstrate that both mechanical tearing of the lamina and biochemical modification of lamin B1 filaments are required for NE breakdown.**

The nuclear lamina is a filamentous meshwork underlying the nucleoplasmic side of the nuclear envelope (NE)<sup>1</sup> (1). The primary components of the nuclear lamina are intermediate filament (IF) lamins and in particular lamin B1, which is constitutively expressed (2, 3). Human lamin B1 mutated by deletion of the rod domain (B1 $\Delta$ rod) causes severe alteration of the nuclear lamina organization (4–6), which suggests that lamin B1 plays a key role in the structural integrity of the NE (7). Lamins and many other NE proteins are subject to mitotic phosphorylation by the Cdc2 kinase, which diminishes protein-protein interactions required for NE integrity, dispersing structural proteins into the cytoplasm at mitosis (8). In partic-

ular, a lamin B1 mutant lacking the Cdc2 kinase phosphorylation site prevents NE breakdown (9–11), which suggests that lamin phosphorylation is a prerequisite for NE destabilization before mitosis (12).

Nevertheless, there is growing evidence *in vitro* and *in vivo* that lamin B1 disassembly is independent of NE breakdown. Lamin B1 solubilization *in vitro* has been shown to occur without NE breakdown (13). Time-resolved fluorescence microscopy reveals that the organization of green fluorescent protein-lamins in the NE of live cells remains intact until NE breakdown and little soluble lamin (<5%) can be detected through fluorescence after recovery before NE breakdown (14). Instead, early spindle microtubules cause folds in the NE, which develop into deep invaginations that create an initial hole in the NE (15). This hole forms at a specific NE position, which is distal from the centrosomes (14). The non-random position of the hole on the NE surface argues against weakening of the lamina by lamin disassembly prior to NE breakdown, which would create randomly located holes wherever lamin is completely disassembled (14). Based on these observations, it has been speculated that mechanical tearing generated by microtubules play the main role in NE breakdown (14).

To investigate whether the microtubule-induced deformation is sufficient for NE breakdown, we assess the viscoelastic properties of lamin B1 to determine the mechanical resilience of a reconstituted lamin B1 network. We focus on lamin B1 because it is the primary component of the NE prior to its breakdown in the G<sub>2</sub>/M transition whereas lamin A/C is dissociated from the NE (15). We use quantitative rheological methods to examine the mechanical response of lamin B1 networks subject to shear and axial deformations similar to those generated by premitotic microtubules. To provide a basis of comparison, we report the mechanical properties of cytoplasmic intermediate filaments vimentin, complex epithelia keratin K5–K14, and simple epithelia keratin K8–K18, as well as F-actin. Our results show that lamin B1 can (even in the absence of auxiliary proteins) form exceptionally resilient structures through strong interfilament interactions. The maximum deformation of the NE generated by early spindle microtubules is much lower than the deformation required to breakdown a lamin B1 network, which suggests that NE breakdown has to involve both mechanical tearing of the lamina and biochemical modifications of lamin filaments.

## MATERIALS AND METHODS

**Lamin B1 Purification and Assembly**—Unless specified, all reagents were purchased from Sigma Chemical Company. Purification of human lamin B1 is based on published protocols (5, 16). Briefly, *Escherichia coli* BL21/DE3 containing a human lamin B1 expression plasmid was grown at 37 °C in 200 ml of SOB medium (20 g of Tryptone, 5 g of yeast extract, 0.5 g of NaCl, 0.186 g of KCl, and 20 mM MgCl<sub>2</sub> per liter H<sub>2</sub>O) supplemented with 50  $\mu$ g/ml kanamycin. Human lamin B1 cDNA was a generous gift from E. C. Schirmer (The Scripps Research Institute).

\* This work was funded by National Science Foundation Grants NIRT CTS0210718 (to D. W.) and DMII-0228246 (to B. W. S.) and NASA Grant NAG9–1563 (to D. W. and Y. T.). The costs of publication of this article were defrayed in part by the payment of page charges. This article must therefore be hereby marked “advertisement” in accordance with 18 U.S.C. Section 1734 solely to indicate this fact.

[S] The on-line version of this article (available at <http://www.jbc.org>) contains additional information and Supplemental Figs. 1–3.

|| To whom correspondence may be addressed: Dept. of Chemical and Biomolecular Engineering, The Johns Hopkins University, 3400 N. Charles St., Baltimore, MD 21218. Tel.: 410-516-7006; Fax: 410-516-5510; E-mail: wirtz@jhu.edu.

\*\* To whom correspondence may be addressed: Dept. of Chemical and Biomolecular Engineering, The Johns Hopkins University, 3400 N. Charles St., Baltimore, MD 21218. Tel.: 410-516-5287; Fax: 410-516-5510; E-mail: yiider@jhu.edu.

<sup>1</sup> The abbreviations used are: NE, nuclear envelope; IF, intermediate filament; F-actin, filamentous actin.

Expression was induced with 1 mM isopropyl-thio- $\beta$ -D-galactopyranoside at  $A_{595}$  0.7 for 4 h at 37 °C. Cells were lysed by sonication in phosphate-buffered saline with 1.5 mM  $\beta$ -mercaptoethanol and protease inhibitor. After a 7-min centrifugation at  $10,000 \times g$ , the pellet was washed with 0.2% Triton X-100 and resuspended in 20 mM Tris, pH 8.0, 300 mM NaCl, 8 M urea, 3 mM  $\beta$ -mercaptoethanol, 0.2 mM phenylmethylsulphonyl fluoride. The solution was then incubated with nickel-nitrilotriacetic acid resin (Qiagen, Gaithersburg, MD) for 45 min and eluted in fractions with the same buffer containing a 0–200 mM imidazole gradient. The eluate was dialyzed in 20 mM Tris, pH 8.0, 8 M urea, 3 mM  $\beta$ -mercaptoethanol, 0.2 mM phenylmethylsulphonyl fluoride and was applied to a Mono Q column (Bio-Rad) eluted with NaCl gradient from 0–1 M. The lamin-rich fraction was examined by SDS-PAGE and further dialyzed into 20 mM Tris, pH 8.0, 8 M urea, 2 mM dithiothreitol, 0.2 mM phenylmethylsulphonyl fluoride for storage. The protein purity was verified to be >99% by SDS-PAGE assay followed by densitometry. For filament assembly, lamin in 8 M urea at 1 mg/ml was dialyzed against 20 mM Tris, pH 8.8, 1 mM EDTA, 1 mM dithiothreitol, 0.2 mM phenylmethylsulphonyl fluoride (5) for 16 h at 4 °C. 150 mM NaCl was added to the solution to induce lamin assembly. Alternatively, dialysis in steps (which is for instance required for keratin (17)) did not affect the structural and mechanical outcomes of lamin B1 networks (data not shown).

**Actin and Vimentin Purification and Assembly**—Actin was prepared from chicken breast (18) with an extra step of gel filtration by Sephacryl S-300 (Sigma) (19). Purified actin was stored as  $\text{Ca}^{2+}$ -actin in continuous dialysis at 4 °C against buffer G (0.2 mM ATP, 0.5 mM dithiothreitol, 0.2 mM  $\text{CaCl}_2$ , 1 mM sodium azide, and 2 mM Tris-HCl, pH 8.0).  $\text{Mg}^{2+}$ -actin filaments were generated by adding 0.1 volume of  $10 \times$  KMEI (500 mM KCl, 10 mM  $\text{MgCl}_2$ , 10 mM EGTA, 100 mM imidazole, pH 7.0) polymerizing salt to 0.9 volume of G-actin in buffer G.

The purification of human vimentin is based on a published protocol (20) using a Mono Q column (Bio-Rad). Human vimentin cDNA was a generous gift from R. D. Goldman (Northwestern University Medical School). To form filaments, vimentin that was solubilized in 1 mM EDTA, 0.1 mM EGTA, 0.1 mM dithiothreitol, and 5 mM Tris-HCl, pH 8.4, was dialyzed into filament buffer (0.1 mM dithiothreitol, 160 mM NaCl, and 25 mM Tris-HCl, pH 7.5) at 37 °C (21).

**Rheology**—The mechanical properties of lamin B1 networks were evaluated using a strain-controlled, cone-and-plate rheometer (ARES-100, TA Instruments, Piscataway, NJ) (19, 22). Shear deformations of controlled amplitude and frequency were applied via precise dynamic rotations of the lower plate; the stress induced within the network was measured through a sensitive torque transducer connected to the upper cone. Lamin B1 solutions were supplemented with 150 mM NaCl and immediately loaded in the space between the cone and plate. Once the cone was set into position, 0.5 mg/ml phosphatidylcholine dissolved in chloroform was applied to the air-water interface to eliminate the interfacial localization of lamins (17). The dead time is estimated to be 5 min before rheological measurements. Gelation was monitored by measuring the time-dependent elasticity of the network. Elasticity was measured by applying two oscillatory deformations of 1% amplitude at a frequency of 1 rad/sec every 30 s until a steady state was attained (~1–3 h). At steady state, the frequency-dependent viscoelastic moduli of the networks,  $G'(\omega)$  and  $G''(\omega)$ , were computed by dividing the in-phase and out-of-phase components of the measured oscillatory stress induced within the network by the applied strain amplitude (here 1%) (19, 22). The viscoelastic nature (*i.e.* viscous *versus* elastic) of lamin networks was characterized by the phase angle  $\delta = \tan^{-1}(G''/G')$ . The response of the lamin networks to shear was assayed by applying oscillatory deformations at 1 rad/s and amplitudes from 0.5 to 500%. For all rheological experiments, the temperature of the solutions was maintained at 25 °C to within 0.1 °C.

## RESULTS

**Mechanical Properties of Reconstituted Lamin B1 Networks**—We tested the mechanical properties of human lamin B1 networks in assembly buffer using quantitative rheological methods as a function of time after onset of assembly and at steady state. Suspensions of lamin B1 (Fig. 1A) were allowed to gel in the space between the cone and plate of the rheometer, and elastic modulus ( $G'$ ) and viscous modulus ( $G''$ ) of the suspensions were probed by 1% oscillatory deformations. The elastic modulus and viscous modulus represent the in-phase and out-of-phase components of the stress induced in the networks normalized by the amplitude of the applied deformation (23,

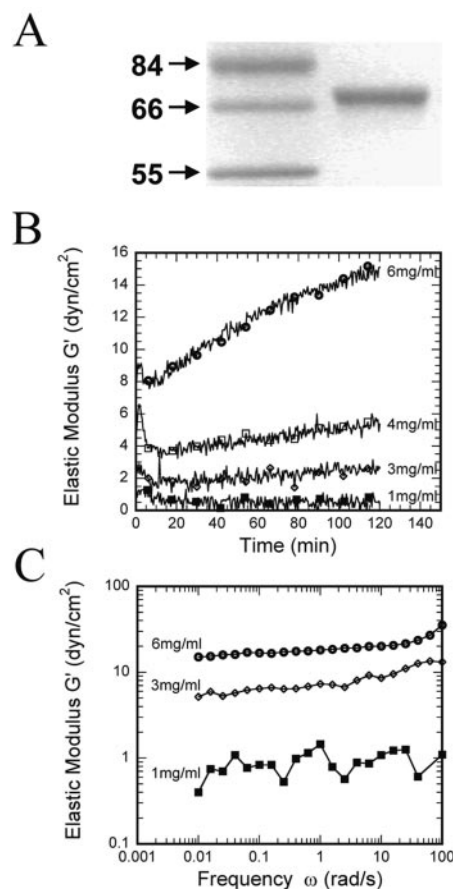
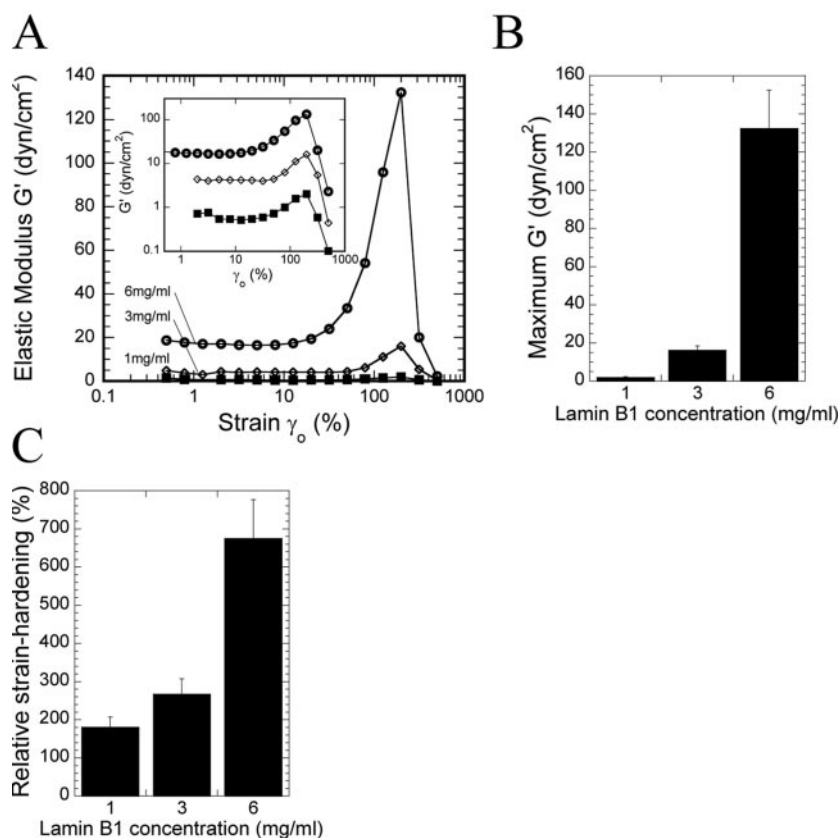


**FIG. 1. Mechanical properties of lamin B1 networks.** A, human lamin B1 was subject to a SDS-PAGE assay to show protein purity. B, increase in elasticity  $G'$  and viscous modulus  $G''$  upon lamin B1 assembly. Lamin concentrations range between 1 and 6 mg/ml in standard assembly buffer.  $G'$  and  $G''$  are the in-phase and out-of-phase components of the stress induced by oscillatory deformations of small amplitude ( $\gamma_0 = 1\%$ ) normalized by the amplitude of the deformations  $\gamma_0$ . Dead time between loading in the rheometer and measurement is 5 min. C, frequency-dependent elasticity  $G'(\omega)$  and viscous modulus  $G''(\omega)$  of lamin B1 networks a steady state for lamin B1 concentrations ranging between 1 and 6 mg/ml.

24). To monitor gelation kinetics, networks were subject to a couple of oscillatory deformations of small 1% amplitude every 30 s until the elasticity of the network reached a steady state value (the first 2 h are shown in Fig. 1B). The elastic modulus of the network dominated rapidly (~5 min) the viscous modulus of the network, an effect measured by the low phase angle  $\delta = \tan^{-1}(G''/G') \sim 10^\circ$  of the network. The phase angle of a material characterizes its viscoelastic nature (24); *e.g.*  $\delta = 90^\circ$  for water or glycerol, which from a rheological point of view corresponds to a liquid-like behavior, and  $\delta \sim 0^\circ$  for a very stiff rubber corresponding to a solid-like behavior. Therefore, rheometry reveals that lamin B1 networks display a pronounced solid-like character.

The rate of gelation, estimated here as the inverse of the time required for attaining 90% of the steady state value (Fig. 1B), increased slightly from  $0.05 \text{ min}^{-1}$  to  $0.125 \text{ min}^{-1}$  for lamin B1 concentrations between 1 and 6 mg/ml. Over that concentration range, the elasticity of lamin B1 networks increased ~15-fold (Fig. 1B). By subjecting lamin B1 networks to small oscillatory deformations of frequencies between  $\omega = 0.01$  and 100 rad/s, we measured the dynamic elasticity,  $G'(\omega)$ , and viscous modulus,  $G''(\omega)$ , of lamin B1 networks (Fig. 1C). The frequency dependence of  $G'(\omega)$  was weak (Fig. 1C), which signifies that for the tested lamin concentrations lamin B1 polymers in solution

**FIG. 2. Strain-induced hardening of lamin B1.** A, dependence of the elastic modulus  $G'$  of lamin B1 suspensions on the deformation amplitude  $\gamma_0$  at different lamin B1 concentrations in standard assembly buffer at 25 °C. *Inset*, associated log-log plot of  $G'(\gamma_0)$  versus  $\gamma_0$ . B, maximum value of elastic modulus,  $G'_{\max}$ , displayed by lamin B1 networks under shear as a function of lamin B1 concentration. C, degree of strain-hardening, SH, of lamin B1 networks, which corresponds to the maximum elasticity of the network under shear relative to the baseline elastic modulus at low strain amplitudes,  $SH = (G'_{\max} - G'_{\text{low } \gamma_0})/G'_{\text{low } \gamma_0}$ .



showed little or no mobility for time scales as long as  $2\pi/\omega \sim 600$ s (Fig. 1C). These results show that (from a rheological point of view) lamin networks behave as cross-linked gels.

**Lamin B1 Networks Strain-harden under Shear**—Up to 1 h prior to NE breakdown, the interphase nucleus is subject to large intracellular mechanical stresses: the NE experiences localized folds and deep invaginations caused by early spindle microtubules before the disassembly of lamin B1 filaments, which occurs only after NE breakdown (14, 15). To test the response of lamin B1 to mechanical stresses such as those created by premitotic microtubules, lamin B1 networks were subject to deformations of fixed frequency of 1 rad/s and amplitude ranging between 0.5 and 500%. Profiles of the strain-dependent elasticity of lamin B1 networks,  $G'(\gamma_0)$ , featured three distinct regions (Fig. 2A).  $G'(\gamma_0)$  was mostly independent of  $\gamma_0$  at low deformation amplitudes, increased dramatically at intermediate strain amplitudes (*i.e.* the network strain-hardens under shear), and declined rapidly at large strain deformations (*i.e.* the network strain-softens under shear) (Fig. 2A and *inset*). The maximum value reached by  $G'(\gamma_0)$  relative to the base line increased greatly with lamin B1 concentration (Fig. 2, B and C). Hence, lamin B1 networks show pronounced strain-hardening, whereby the network stiffens under shear.

To further investigate the effect of shear deformations on lamin B1 networks, oscillatory deformations of the type  $\gamma(t) = \gamma_0 \sin \omega t$  of fixed frequency ( $\omega = 1$  rad/sec) and increasing deformation amplitude  $\gamma_0$  were applied to the networks, and the resulting induced stress  $\sigma(t)$  was monitored as a function of time (Fig. 3A). Up to a strain amplitude of  $\sim 20\%$ ,  $\sigma(t)$  was a periodic function (Fig. 3A). However, past that threshold strain amplitude,  $\sigma(t)$  became a non-periodic function with a maximum stress that declined from one shear cycle to the next (Fig. 3C). For small deformations, lissajous figures of  $\sigma(t)$  versus  $\gamma(t)$  displayed a narrow ellipse (Fig. 3B), which indicates that little viscous dissipation within the network occurred during shear (*i.e.* the network is much more elastic than viscous). For large

deformation amplitudes, lissajous figures displayed a wide ellipse (Fig. 3D) with a major axis slightly rotating clockwise because the network softened during the shear cycles. This figure shows that the stress increased faster than linearly with the strain (arrow in Fig. 3D), another hallmark of shear-induced hardening in lamin networks (25).

**Lamin Displays Exceptional Resilience against Mechanical Stresses**—Next, we investigated the intrinsic mechanical resilience of lamin, *i.e.* the largest deformation that lamin can sustain before its ultimate breakdown. The resilience of lamin B1 networks, *i.e.* the strain amplitude at which  $G'$  began to decrease, was extraordinarily high ( $\gamma_0 \sim 200\%$ ) and mostly independent of concentration (Fig. 4). In contrast, our analysis of images of nuclei undergoing large deformations in premitotic cells reported in Ref. 14 shows that the relative shear deformation of the NE created by spindle microtubules does not exceed 13% (see analysis in supplemental material). This is because the seemingly large, micron-scale deformations of the NE occur over the thin ( $\sim 50$ – $100$  nm) lamina thickness. Note that the NE is subject to both shear and axial (*i.e.* extensional) deformations. We computed a maximum axial resilience between 133 and 200% (see supplemental material) whereas the relative axial deformation of the NE *in vivo* was reported to be  $\sim 50\%$  (14). Hence, the (axial or shear) deformations that the lamin network can sustain before breakdown are much larger than deformations caused by microtubules prior to NE breakdown.

Lamin B1 networks are somewhat less elastic but are significantly more solid-like and more resilient than F-actin networks (Fig. 5, A–D). Lamin B1 displays much more pronounced strain-induced hardening than any other network of major cytoskeleton polymer (Fig. 5C). Besides strain-hardening, lamin B1 networks display mechanical properties (elasticity, phase angle, etc.) that are quite similar to those of networks of simple-epithelial keratin K8–K18, complex-epithelial keratin K5–K14, and vimentin (Fig. 5, A–D), all cytoplasmic interme-

**FIG. 3. Mechanical response of lamin B1 networks subject to oscillatory deformations.** *A*, imposed oscillatory shear deformation ( $\gamma(t)$ , open symbols) and induced time-dependent stress ( $\sigma(t)$ , closed symbols). Lamin B1 networks (3 mg/ml) in polymerization buffer at 25 °C were subject to sinusoidal deformations of the type  $\gamma(t) = \gamma_0 \sin \omega t$  of fixed frequency  $\omega = 1$  rad/sec and deformation amplitude of  $\gamma_0 = 10\%$ . *B*, lissajous figure of  $\sigma(t)$  versus  $\gamma(t)$  for  $\gamma_0 = 10\%$ . Same conditions as in *A*. *C*, time-dependent strain ( $\gamma(t)$ , open symbols) and induced stress ( $\sigma(t)$ , closed symbols) with  $\gamma_0 = 100\%$ . Same conditions as in *A*. *D*, lissajous figure for  $\gamma_0 = 100\%$ . Same conditions as in *A*. Arrow indicates change in stress versus strain.

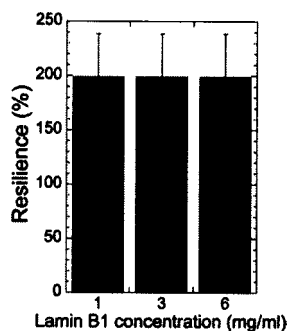
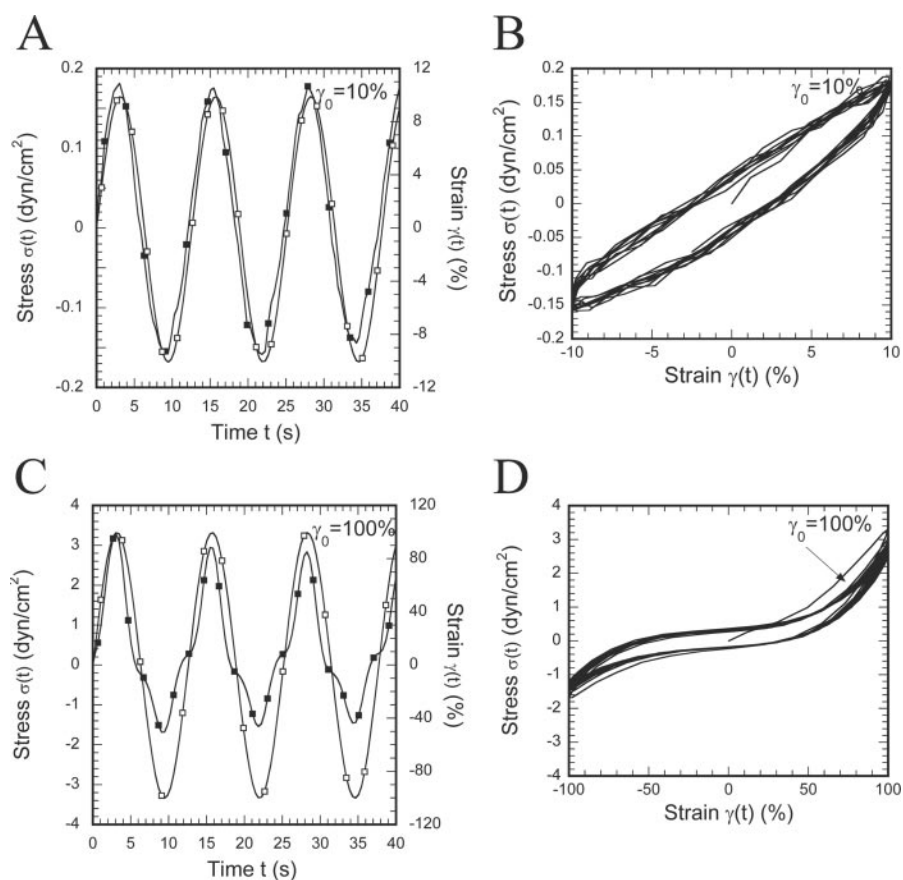


**FIG. 4. Mechanical resilience of lamin B1.** Resilience of lamin B1 networks as a function of lamin B1 concentration. The resilience is the maximum possible deformation of lamin before breakdown, *i.e.* before its elasticity begins to drop when sweeping from low to high deformation amplitude.

diate filaments with well established structural function (17, 26, 27).

#### DISCUSSION

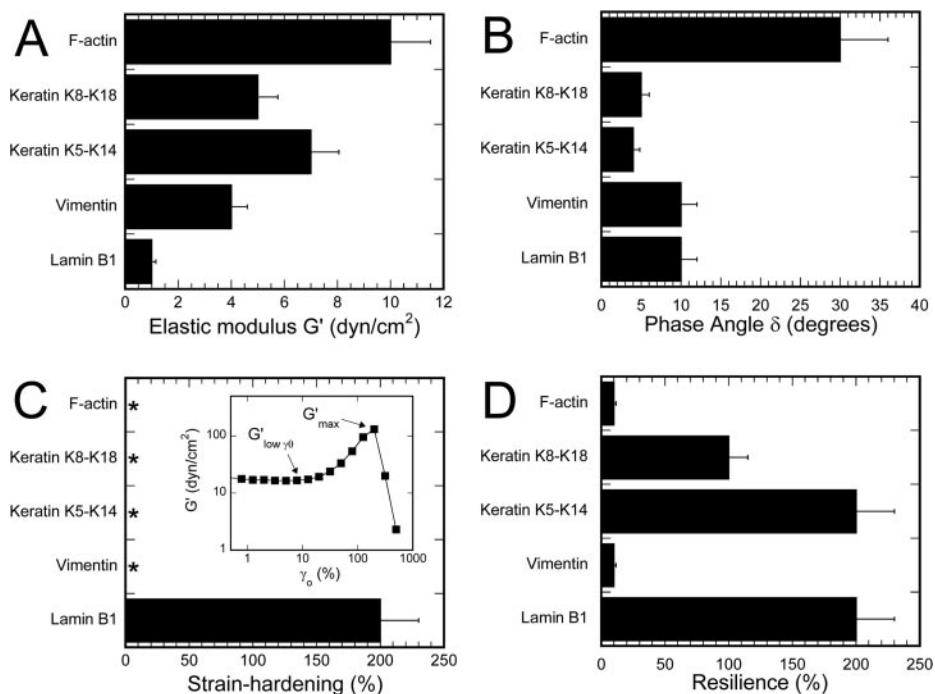
To investigate whether mechanical tearing of the NE by spindle microtubules impinging on the nucleus is the sole mechanism required for NE breakdown, we assessed the viscoelastic properties of lamin B1, the primary component of NE lamina. Using quantitative rheological methods, we measured the mechanical properties of lamin B1 networks subject to different types of shear stresses at broad range. Lamin B1 polymers form remarkably solid-like and resilient structures. Under tension, lamin B1 networks display a pronounced strain-hardening behavior whereby the elasticity of the network increased under shear. The maximum shear that lamin B1 can sustain before breakdown is significantly greater than the deformation caused by spindle microtubules impinging on the NE in prophase. Therefore, mechanical tearing of the lamin

B1-rich lamina is necessary but not sufficient to induce NE breakdown.

**Concentration Dependence of Network Elasticity**—Over the range of concentrations in lamin B1 probed here, the increase in elasticity is compatible with a power law of the type  $G'(c) \sim c^{1.4}$ , where  $c$  is the concentration in lamin B1. A similar concentration dependence of  $G'$  is observed for the stereotypical semiflexible cytoskeleton polymer F-actin (28). Polymer physics theory predicts that the elastic modulus of networks of semiflexible polymers should scale as  $G'(c) \sim c^{1.4}$ , whereas rigid polymers should scale as  $G'(c) \sim c^1$  and flexible polymers should scale as  $G'(c) \sim c^{2.25}$  (29). Thus, our rheological data suggest that lamin B1 polymers in solution are semiflexible polymers, *i.e.* their persistence length (which measures the bending rigidity of the polymer) is of the same order of magnitude as their contour length, which also is the case of cytoplasmic intermediate filaments (30, 31). Compounding the effect of interfilaments interactions, this putative rigidity would provide lamin B1 with a supplemental mechanism to entangle easily and therefore form stiff gels (32, 33).

Lamin B1 networks stiffen under shear stress, *i.e.* they readily display strain-hardening, which potentially stems from the self-interactions that are also responsible for their solid-like character and extraordinary resilience against shear deformations. Under large shear deformations, lamin B1 filaments would be forced to bend while pushing against the topological constraints created by entanglements with other filaments, an effect that is energetically unfavorable. If non-steric interactions were absent, lamin B1 filaments would be able to relax the stress by sliding past one another. Here, for lamin B1 networks, these non-steric interactions impede such sliding motion, which prevents stress relaxation and induces strain-hardening as well as enhanced mechanical resilience. Similarly to actin networks, the presence of other components

**FIG. 5. Mechanical properties of lamin B1 suspensions: comparison with networks of F-actin, complex epithelial IF keratin K4–K14, simple epithelial IF keratin K8–K18, and IF vimentin.** *A*, elasticity,  $G'$ . *B*, phase angle,  $\delta$ . *C*, degree of strain-hardening, SH =  $(G'_{\max} - G'_{\text{low } \gamma_0})/G'_{\text{low } \gamma_0}$ . *Inset*, definition of  $G'_{\max}$  and  $G'_{\text{low } \gamma_0}$ . *D*, resilience against shear. (See definitions in the text.) Note that vimentin and keratin networks display strain-hardening under shear, albeit delayed in strain amplitude and with a maximum elasticity that is lower than the baseline elasticity at low strain amplitudes (17, 39, 42). Hence, SH = 0 (denoted by asterisks in *C*) for those IF networks because  $G'_{\max} = G'_{\text{low } \gamma_0}$ . Data for keratin taken from Ref. 17 and from Ref. 35 for F-actin. The concentration of the solutions is 1 mg/ml.



in the prophase lamina, such as LAP2 $\beta$  and POM121 (which associate with lamin B1 (14)), could further increase the resilience and strain-hardening of lamin B1 meshwork.

*Microtubule-driven Deformation Force Alone Is Insufficient to Break Down Lamin Network*—Unlike the two major cytoskeletal polymers F-actin and microtubule (34, 35), lamin B1 has a natural tendency to generate inter-filament interactions and form bundles even in the absence of auxiliary proteins (1, 13, 16, 36–38). These non-steric interactions promote the formation of large condensed microstructures and bundles and endow lamin B1 polymers with a propensity to form elastic gels. The stiffness and relative magnitude of elastic and viscous moduli of lamin B1 filament suspensions are conspicuously similar to those obtained with reconstituted networks of cytoplasmic intermediate filaments, including vimentin, complex epithelial keratin K4–K14, and simple epithelial keratin K8–K18 (17, 39). The strong solid-like character of IF networks, not shared by the two other major cytoskeleton polymers, originates from strong non-steric interactions between polymers (24). This characteristic allows lamin B1 networks to possess extraordinary shear resilience, exceeding that of microtubule and F-actin networks. We recently measured the micro-mechanical properties of the interphase nucleus *in vivo* (40). These measurements show an intranuclear elastic modulus that is much higher than the viscous modulus, and an elasticity similar to that observed here with reconstituted lamin B1 networks.

When spindle microtubules impinge on the NE, the NE is subject to both shear and axial deformations. One can easily compute the axial resilience from the measured shear resilience. If we assume plane stress conditions and a linear isotropic brittle material we may relate the extensional deformation at failure,  $\epsilon_u$ , to the shear deformation at failure,  $\gamma_u$ , by the Poisson's ratio,  $\nu$ , of the material,  $\epsilon_u = \gamma_u/(1+\nu)$  (see supplemental material). Although  $\nu$  is generally regarded to be  $\sim 0.3$  for gels and polymer networks, we may bound it between an incompressible material ( $\nu = 0.5$ ) and a perfectly compressible material ( $\nu = 0$ ) to conclude that  $2/3\gamma_u \leq \epsilon_u \leq \gamma_u$ , or  $133\% < \epsilon_u < 200\%$ . Thus the maximum axial deformation of lamina before breakdown is much larger than that of the NE before breakdown observed *in vivo*,  $\sim 50\%$  (14).

*The Exceptional Mechanical Resilience of Lamin Imposes the Existence of a Crucial Biochemical Step before NE Breakdown*—The low elastic modulus of lamin B1 will allow relatively large deformations of the lamina created by spindle microtubules as observed *in vivo*, but the extremely high resilience of lamin B1 will prevent its collapse. It might be the 42-residue insert within the lamin rod domain that makes the lamin filament networks mechanically tougher than cytoplasmic IF networks (39), a hypothesis that we shall test in the future. The high resilience of lamin networks stems from both the high resistance of lamin against longitudinal deformation (30, 31) as well as the propensity of lamin filaments to cross-link, a property shared to a lesser extent by other intermediate filaments. The maximum deformation that a lamin B1 network can sustain before breakdown is much greater than the deformations generated by spindle microtubules impinging on the NE. These results together with the fact that lamin B1 depolymerizes only after NE breakdown suggest that NE breakdown by mechanical tearing of the lamina cannot occur until the lamin B1 network is weakened by biochemical modification. Reduction of the homotypic affinity between lamin B1 filaments would greatly diminish the mechanical resilience of the lamina but would not necessarily affect lamin dynamics, solubility, and apparent organization. Therefore, it would not be detected by changes in fluorescence after recovery or total fluorescence intensity (14). The reduction of lamin interfilament interactions before NE breakdown could be achieved by premitotic phosphorylation of lamin B1 or by regulatory proteins that are yet to be identified. The lamina contains many more components besides lamin B1, including nuclear actin and protein 4.1 (41), which form filamentous structures that could further enhance the resilience of lamina.

*Acknowledgment*—We thank Dr. E. C. Schirmer (The Scripps Research Institute) for his generous gift of human lamin B1 cDNA.

#### REFERENCES

1. Aebi, U., Cohn, J., Buhle, L., and Gerace, L. (1986) *Nature* **323**, 560–564
2. Hoger, T. H., Zatloukal, K., Waizenegger, I., and Krohne, G. (1990) *Chromosoma (Berl.)* **100**, 67–69
3. Zewe, M., Hoger, T. H., Fink, T., Lichter, P., Krohne, G., and Franke, W. W. (1991) *Eur. J. Cell Biol.* **56**, 342–350
4. Foissner, R., and Gerace, L. (1993) *Cell* **73**, 1267–1279
5. Schirmer, E. C., Guan, T., and Gerace, L. (2001) *J. Cell Biol.* **153**, 479–489

6. Furukawa, K., Fritze, C. E., and Gerace, L. (1998) *J. Biol. Chem.* **273**, 4213–4219
7. Gruenbaum, Y., Wilson, K. L., Harel, A., Goldberg, M., and Cohen, M. (2000) *J. Struct. Biol.* **129**, 313–323
8. Ward, G. E., and Kirschner, M. W. (1990) *Cell* **61**, 561–577
9. Heald, R., and McKeon, F. (1990) *Cell* **61**, 579–589
10. Peter, M., Nakagawa, J., Doree, M., Labbe, J. C., and Nigg, E. A. (1990) *Cell* **61**, 591–602
11. Peter, M., Heitlinger, E., Haner, M., Aebi, U., and Nigg, E. A. (1991) *EMBO J.* **10**, 1535–1544
12. Buendia, B., and Courvalin, J. C. (1997) *Exp. Cell Res.* **230**, 133–144
13. Newport, J., and Spann, T. (1987) *Cell* **48**, 219–230
14. Beaudouin, J., Gerlich, D., Daigle, N., Eils, R., and Ellenberg, J. (2002) *Cell* **108**, 83–96
15. Georgatos, S. D., Pyrasopoulou, A., and Theodoropoulos, P. A. (1997) *J. Cell Sci.* **110**, 2129–2140
16. Karabinos, A., Schunemann, J., Meyer, M., Aebi, U., and Weber, K. (2003) *J. Mol. Biol.* **325**, 241–247
17. Yamada, S., Wirtz, D., and Coulombe, P. A. (2003) *J. Struct. Biol.* **143**, 45–55
18. MacLean-Fletcher, S. D., and Pollard, T. D. (1980) *J. Cell Biol.* **85**, 414–428
19. Tseng, Y., Fedorov, E., McCaffery, J. M., Almo, S. C., and Wirtz, D. (2001) *J. Mol. Biol.* **310**, 351–366
20. Moir, R. D., Donaldson, A. D., and Stewart, M. (1991) *J. Cell Sci.* **99**, 363–372
21. Herrmann, H., Haner, M., Brettel, M., Muller, S. A., Goldie, K. N., Fedtke, B., Lustig, A., Franke, W. W., and Aebi, U. (1996) *J. Mol. Biol.* **264**, 933–953
22. Tseng, Y., and Wirtz, D. (2001) *Biophys. J.* **81**, 1643–1656
23. Ferry, J. D. (1980) *Viscoelastic Properties of Polymers*, John Wiley and Sons, New York
24. Coulombe, P. A., Bousquet, O., Ma, L., Yamada, S., and Wirtz, D. (2000) *Trends Cell Biol.* **10**, 420–428
25. Ma, L., Xu, J., Coulombe, P. A., and Wirtz, D. (1999) *J. Biol. Chem.* **274**, 19145–19151
26. Janney, P. A., Euteneuer, U., Traub, P., and Schliwa, M. (1991) *J. Cell Biol.* **113**, 155–160
27. Rogers, K. R., Eckelt, A., Nimmrich, V., Janssen, K. P., Schliwa, M., Herrmann, H., and Franke, W. W. (1995) *Eur. J. Cell Biol.* **66**, 136–150
28. Palmer, A., Xu, J., Kuo, S. C., and Wirtz, D. (1999) *Biophys. J.* **76**, 1063–1071
29. Morse, D. C. (1998) *Macromolecules* **31**, 7044–7067
30. Mucke, N., Kreplak, L., Kirmse, R., Wedig, T., Herrmann, H., Aebi, U., and Langowski, J. (2004) *J. Mol. Biol.* **335**, 1241–1250
31. Fudge, D. S., Gardner, K. H., Forsyth, V. T., Riekel, C., and Gosline, J. M. (2003) *Biophys. J.* **85**, 2015–2027
32. Panorchan, P., Wirtz, D., and Tseng, Y. (2004) *Phys. Rev. E.*, in press
33. Heidemann, S. R., and Wirtz, D. (2004) *Trends Cell Biol.* **14**, 160–166
34. Sato, M., Schwartz, W. H., Selden, S. C., and Pollard, T. D. (1988) *J. Cell Biol.* **106**, 1205–1211
35. Xu, J., Tseng, Y., and Wirtz, D. (2000) *J. Biol. Chem.* **275**, 35886–35892
36. Gieffers, C., and Krohne, G. (1991) *Eur. J. Cell Biol.* **55**, 191–199
37. Heitlinger, E., Peter, M., Lustig, A., Villiger, W., Nigg, E. A., and Aebi, U. (1992) *J. Struct. Biol.* **108**, 74–89
38. Moir, R. D., Spann, T. P., Herrmann, H., and Goldman, R. D. (2000) *J. Cell Biol.* **149**, 1179–1192
39. Ma, L., Yamada, S., Wirtz, D., and Coulombe, P. A. (2001) *Nat. Cell Biol.* **3**, 503–506
40. Tseng, Y., Lee, J. S., Kole, T. P., Jiang, I., and Wirtz, D. (2004) *J. Cell Sci.* **117**, 2159–2167
41. Krauss, S. W., Chen, C., Penman, S., and Heald, R. (2003) *Proc. Natl. Acad. Sci. U. S. A.* **100**, 10752–10757
42. Bousquet, O., Ma, L., Yamada, S., Gu, C., Idei, T., Takahashi, K., Wirtz, D., and Coulombe, P. A. (2001) *J. Cell Biol.* **155**, 747–754